Journal of Sound and Vibration (1998) **212**(2), 187–214

NOISE SHIELDING EFFICIENCY IN AN URBAN SYSTEM

E. Walerian and R. Janczur

Institute of Fundamental Technological Research, Polish Academy of Sciences, Swietokrzyska 21, 00-049 *Warsaw, Poland*

(*Received* 20 *July* 1994, *and in final form* 24 *November* 1995)

To estimate the shielding efficiency of buildings, a model which simulates noise propagation in an urban area has been used. The simulation model assumes the equivalent highway model where vehicles are replaced by equivalent point sources which emit typical traffic noise. Interactions of acoustical waves with obstacles, on the path from the source to the observation point, are reduced to specular reflections from surfaces and diffraction at edges (wedges) of obstacles. The prepared PROP3 computer program allows estimation of sound equivalent level in dB(A) at the observation point in a built-up area, for a highway of known vehicles rate flow and vehicle average speed.

1. INTRODUCTION

An obstacle's efficiency as a noise control measure depends on the obstacle itself and its interactions with the environment. Generally, these interactions cause degradation of the obstacle's shielding efficiency [1].

In order to solve the noise abatement problems in urban areas, a model of environmental noise, which can be used for simulation of waves propagation from a source through a space with obstacles, has to be prepared. Elementary phenomena can be treated: spreading of the acoustical wave in the space; interaction of the acoustical wave with obstacles. On the assumption that the spreading occurs in an ideal medium at rest, with the medium inhomogeneity and weather conditions ignored, the main attention may be focused on the multiple interactions with obstacles.

There have been several theoretical attempts to describe the wave interaction with obstacles [2–7]. Some practical approximations have also been proposed, especially for noise abatement problems [8–21].

For an urban area where, the dimensions of buildings are large enough in relation to the length of the wave dominant in the noise spectrum, a high frequency approximation of diffraction phenomena is justified. Thus, to describe the multiple interactions with obstacles the total acoustical field can be divided into geometrical and diffraction parts [4, 22]. According to this, in the paper, the wave interaction with obstacles which are composed of limited panels, is divided into transmission through panels, reflections from panels, and diffraction at edges and/or wedges.

In a half-space with obstacles representing an urban system, the total acoustical field contains a sum of parallel chains of the elementary interactions, where each chain describes the different wave path to the observation point. The geometrical part, calculated by use of the image method, is widely applied for description of the acoustical field in bounded

0022–460X/98/170187 + 28 $25.00/0/sv951439

spaces [23–29]. The addition of diffraction smooths the field and offers a more precise physical description.

Generally, the most important components in the acoustical energy calculation are the first few reflections. The diffraction is introduced into the propagation model to make the total field smooth at the boundaries of shadow and reflection waves, where the acoustical pressure is zero and its level tends to minus infinity. The smooth field is just obtained at the stage of summation of the first order interactions. It is also possible that a smooth field can be obtained only after summation of reflections up to large enough order but computation time increases.

The description of diffraction [30–33] used here is in a form which contains an undisturbed wave times the diffraction coefficient. Of the same form are descriptions of transmission and reflection, taking into account that for the reflection the undisturbed wave is emitted by the image source. Thus, all of the three kinds of interactions can be used as elements to build a chain of interactions to which the wave is subjected to on its path from the source to the observation point. The chain can contain an arbitrary number of interactions in an arbitrary sequence (see sections 2.2, 2.3).

By comparison with experimental data [34, 35], it has been found that the adopted description of diffraction works up to a source (or observation point) distance from the wedge of wavelength order. Also, by comparing the description of double diffraction at the building wedges with the description which uses the Keller theory [36], an acceptable accordance has been found.

The accuracy of the propagation model, which depends on the description of elementary interactions (transmission, reflection, diffraction) and on the assumed upper order of interactions $\mathscr{K}$, has been tested on scale indoor experiments [37, 38]. In both cases the interactions in a system which comprises the ground, a plane screen and a building facade have been investigated. The screen and facade were parallel; thus, depending on the order of interactions, all possible sequences of interactions were present. The first series of experiments [37] has been performed in the frequency domain, with use of the diffraction description coming from the asymptotic expression of the MacDonald solution [4]. The second series [38] has been carried on in the time domain, with the expression for diffraction given according to the Rubinowicz theory [39]. Both applied diffraction theories lead to a description of the action of a secondary source at a wedge.

The general noise model prepared [33] comprises the source model, which can be constructed by a unit simple harmonic point source, and the propagation model, which can simply be identified as the system transfer function. The noise model can be used for all systems for which the high frequency approximation is an appropriate one, and where transmissions, reflections from panels and diffractions at their wedges are the predominant processes.

In preparing the environmental noise model for a built-up area, a special model for the highway as the predominant noise source in an urban area is introduced (section 2.1). It is constructed of the equivalent point sources representing the individual vehicles moving along a highway.

Based on the environmental noise model for a built-up area, the PROP3 simulation program has been prepared [30–32]. The propagation model is adjusted to obstacles (buildings) whose shape can be approximated by a shoe-box. Plane acoustical screens are also included. Double diffraction at parallel building wedges and at the edges of two parallel screens are taken into account.

In the PROP3 simulation program, the adequacy of the urban system description and adequacy of a highway model is comparable with the adequacy in the scale model investigations of a relatively large urban segment, with scale factor of order 1:100 [40, 41].

The similar simulation program, which, in the propagation model, includes transmission and reflection (described by image sources) and diffraction according to the Keller theory (with the assumed ray tracing method), has been proved experimentally [42]. The noise propagation model used in the paper is of a more general character. It is self-consistent as both reflection and diffraction are related to image points representing the secondary sources of reflection and diffraction waves. The description of diffraction differs from the Keller geometrical theory in that it is related to the undisturbed wave at the observation point while in the Keller theory it is related to the incident wave at the wedge. As the Keller diffraction theory is an extension of the ray tracing theory, the description presented here can be treated as an extension of the image method.

In this paper (section 3), the PROP3 computer program has been used to calculate the shielding efficiency of a single building and the first row of buildings along a highway. It is shown how it changes when a stationary source has been replaced by the moving one.

In the case of a single building, the influence on the building shielding efficiency of the building's limited length, presence of the ground, and the additional plane behind the observation points (representing a facade of protected buildings) has been investigated.

In the case of the first row of buildings along a highway, the urban system geometry (highway position, building dimensions and positions) are decisive factors. The shielding efficiency is presented for variable angles created by buildings with the highway axis while the other parameters are kept constant.

The examples presenting the shielding efficiency of a row of buildings have been published [39–42]. In these papers only the geometrical part of the acoustical field has been taken into consideration. In references [39–41], the additional, empirically established attenuation during propagation in the medium is included. A moving point source representing a car and a planar projection of buildings on the plane perpendicular to the highway lane has been taken. Thus, reflections between buildings have been omitted. These effects have been included in reference [42] where only the single moving source representing a vehicle has been examined.

2. THE ENVIRONMENTAL NOISE MODEL

In order to solve the noise abatement problem in an urban area a model of environmental noise, providing a procedure for the sound equivalent level calculation, is needed. Formally, it can be presented in the form

$$L_{eq}(\mathrm{dB(A)}) = \hat{\Pi}_0(\ldots)\hat{\Pi}(\ldots)Q(\ldots), \tag{1}$$

where the source model is represented by $Q(\ldots)$, the operator $\hat{\Pi}(\ldots)$ describes wave propagation, and the operator $\hat{\Pi}_0(\ldots)$ the human perception.

It has been widely discussed how to determine the noise annoyance objectively. Despite all doubts, following the ISO recommendation, the sound equivalent level is used for rating the annoyance in legislation. Thus, the operator $\hat{\Pi}_0(\ldots)$, acting on the acoustical pressure coming from the action of the propagation operator on the source (equation (1)), should give the sound equivalent level. In the time domain the sound equivalent level is defined by the time average

$$L_{eq}(\mathrm{dB(A)}) = 10 \log \left\{ \frac{1}{T} \int_{-T/2}^{T/2} [p_A^2(t)/p_0^2] \, \mathrm{d}t \right\}, \tag{2}$$

$$p_0 = 2 \times 10^{-5} \, \mathrm{N/m^2}, \tag{3}$$

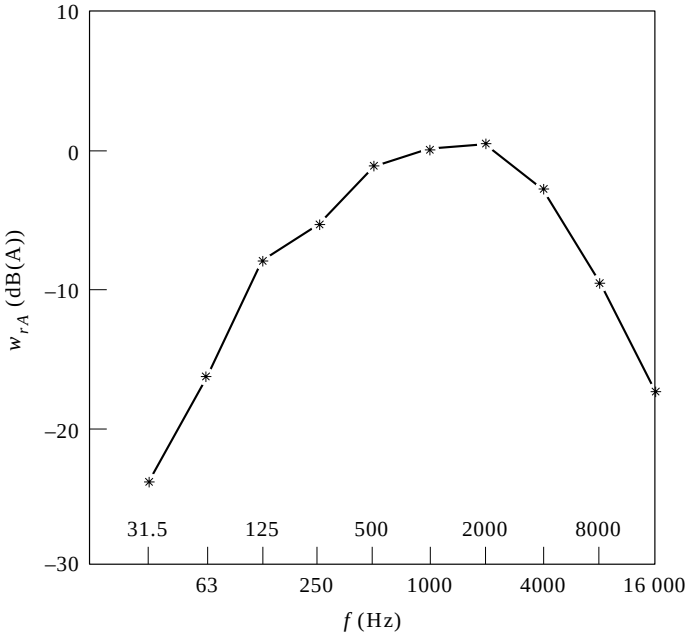

Figure 1. The average, A-weighted, relative power spectrum of traffic noise [44].

where $p_A(t)$ is the A-weighted sound pressure observed at the observation point during the time interval T. In the frequency domain this means calculations of the A-weighted mean sound energy level (see section 2.1).

2.1. A HIGHWAY AS A NOISE SOURCE

A highway is a complex noise source, composed of individual vehicles moving along highway lanes. The equivalent source of individual vehicles is assumed to be an omnidirectional point source, at the height above the ground of 0·7 m [43], which radiates into a homogeneous, loss-free atmosphere at rest. It is assumed to emit noise of the average traffic noise spectrum (see Figure 1) [44]. From empirical data, the differences between the equivalent sources of light and heavy vehicles can be introduced by taking for them different spectra and heights above the ground.

By adopting a concept of sound exposure [45–49] to a drive-by of a vehicle, the highway model as a noise source is assumed. For freely flowing traffic of the total average flow rate N (vehicles/h), represented by the equivalent sources moving, along J lanes parallel to the

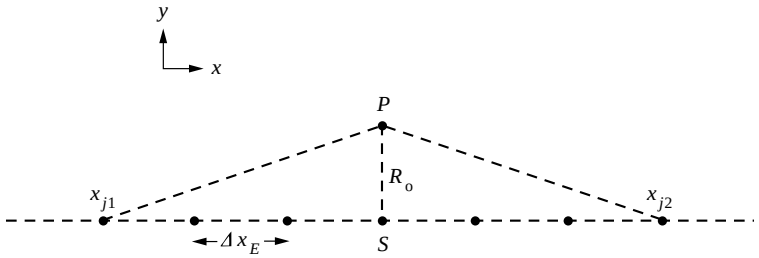

Figure 2. The point source locations along the highway lane segment.

x-axis (see Figure 2), with average speed v (m/h), the sound equivalent level of the highway segment is obtained:

$$L_{eq}(T = 1\text{ h})(\text{dB(A)}) = 10 \log \sum_{j=1}^{J} N_j E_{Aj}/p_0^2. \tag{4}$$

Here N_j is the vehicle rate flow on each j-lane,

$$N_j = N/J. \tag{5}$$

The quantity E_{Aj} is the A-weighted average sound energy, emitted during the drive-by of the j-lane segment by a single equivalent source; thus

$$N_j E_{Aj} = N_j \int_{-t/2}^{t/2} p_{Aj}^2(t)\,\mathrm{d}t = \frac{1}{\Delta x} \int_{x_{j1}}^{x_{j2}} p_A^2(x_j)\,\mathrm{d}x_j, \tag{6}$$

where

$$\Delta x = v/N_j\ (m/\text{vehicles}) \tag{7}$$

is the average spacing between successive vehicles on the j-lane segment of length $(x_{j2} - x_{j1})$.

In equation (6), although the sound exposure is defined for $t \to \infty$, finite boundaries are introduced. When as a limitation criterion it is assumed that the sound level at the observation point P due to the source at the ends of the j-lane (x_{j2}, x_{j1}) is 10 dB lower than that due to the source at the smallest distance R_0 to the observation point P (see Figure 2), then

$$(x_{j2} - x_{j1}) = 6R_0 \tag{8}$$

To obtain the equivalent sound level the integration in equation (6) has to be executed. Analytically this can only be done for free space when there are no buildings. In other cases the integration has to be replaced by discrete summation, then

$$N_j E_{Aj} = \frac{1}{\Delta x} \sum_{u_j=1}^{U_j} p_A^2(u_j \Delta x_E)\Delta x_E. \tag{9}$$

Now, the equivalent sound level is expressed by

$$L_{eq}(T = 1\text{ h})((\text{dB(A)}) = 10 \log \frac{\Delta x_E}{\Delta x} + SL_U. \tag{10}$$

where

$$SL_U = 10 \log \sum_{j=1}^{J} \sum_{u_j=1}^{U_j} p_A^2(u_j \Delta x_E)/p_0^2 = 10 \log \sum_{u=1}^{U} p_A^2(\mathbf{R}_u)/p_0^2, \tag{11}$$

$$U = \sum_{j=1}^{J} U_j = \sum_{j=1}^{J} (x_{j2} - x_{j1})/\Delta x_E. \tag{12}$$

The quantity SL_U represents the sound level due to the set of U stationary equivalent sources at $S_u(x_{j1} + u_j \Delta x_u,\ y_j,\ 0{\cdot}7\ \mathrm{m})$, $j = 1, \ldots, J$. At the observation point $P(x, y, z)$ it is a function of vectors:

$$\mathbf{R}_u = \mathbf{R}_u(\Delta x_u, \Delta y_u, \Delta z_u), \qquad \Delta x_u = x_{j1} + u_j \Delta x_E - x, \tag{13, 14}$$

$$\Delta y_u = y_j - y, \qquad \Delta z_u = 0{\cdot}7m - z. \tag{15, 16}$$

It is obvious that the value of L_{eq} calculated according to equation (10) depends on the choice of the Δx_E value; the smaller is Δx_E the more accurate is the value of L_{eq}. As the upper limit it can be taken that

$$\Delta x_E = \Delta x, \tag{17}$$

where Δx is the average spacing between vehicles on the j-lane (see equation (7)).

With the relative, A-weighted power level of the spectrum of the equivalent source in ten octaves defined as

$$w_{rA}(f_w = \omega_w/2\pi)(\mathrm{dB(A)}) = 10 \log [W(f_w)/W_0] - 10 \log [W(f = 1\ \mathrm{kHz})/W_0] - \Delta L_A, \tag{18}$$

where ΔL_A is the A-weighting correction, the sound level generated by the set of U equivalent sources can be calculated:

$$SL_U(\mathrm{dB(A)}) = 10 \log \sum_{w=1}^{10} 10^{0{\cdot}1 w_{rA}(f_w)} w_U(f_w) + SPL(R = 1\ \mathrm{m}, f = 1\ \mathrm{kHz}), \tag{19}$$

where $SPL\,(R = 1\ \mathrm{m}, f = 1\ \mathrm{kHz})$ is the sound pressure level in the 1 kHz band at a distance of 1 m from the equivalent point source.

In the w-octave-band of centre frequency f_w, the factor $w_U(f_w)$ represents the acoustical energy of the set of U unit point sources emitting simple harmonic waves of frequencies $f_{ws} \in \langle F_{w1}, F_{w2} \rangle$:

$$w_U(f_w) = \frac{1}{S_w} \sum_{s=1}^{S_w} \sum_{u=1}^{U} |p(R_u, f_{ws})|^2. \tag{20}$$

The number S_w of simple harmonic frequencies f_{ws} in the $\langle F_{w1}, F_{w2} \rangle$ octave-band can be adjusted to the bandwidth or kept constant for all bands. Herein, the second option is applied.

2.2. NOISE PROPAGATION THROUGH AN URBAN AREA

To have an explicit expression for the sound equivalent level (equations (10–20)) the sound pressure $p(R_u, f_{ws})$ is needed. This pressure is identical with the transfer function of an urban system, and is provided by the propagation model (equation (1)) as

$$p(R_u, f_{ws}) = p(S, P) = \hat{\Pi}(\ldots) Q(S). \tag{21}$$

This relation represents the acoustical pressure, at the observation point P, due to a unit simple harmonic point source $Q(S)$ at S, after propagation through a built-up area.

The operator $\hat{\Pi}(\ldots)$ which describes propagation in an urban area has to be found. Since propagation is assumed in an ideal medium with disregard of the air attenuation, and that the acoustical pressure is given in front of a building facade, omitting transmission through a building facade into a room, the problem is limited to description of interactions with obstacles.

The urban system under consideration is represented by a half-space with obstacles. The obstacles are modelled by panels. A plane acoustical screen is represented by a single panel. The buildings are approximated by shoe-boxes.

When the dimensions of the obstacles and their mutual separation distances are large in relation to the wavelength predominant in the A-weighted noise spectrum, the large distance approximation ($kR \gg 1$) is justified. Then interaction with obstacles constructed of panels can be divided into reflection and transmission through a panel, treated here as an unlimited one, and diffraction at the wedges (edges) [4, 22]. Thus, the operator $\hat{\Pi}(\ldots)$ (equation (21)) contains the sum of the parallel chains of the elementary interactions of transmission, reflection and diffraction at wedges (edges). Each i-chain describes the different wave paths to the observation points.

The operator $\hat{T}(S, P)$ describes a spreading in the empty space. When it acts on the simple harmonic source $Q(S)$ of unit strength, at point S,

$$\hat{T}(S, P)Q(S) = \frac{\exp[ikR(S, P)]}{R(S, P)}, \tag{22}$$

then it gives an undisturbed spherical wave at the observation point P.

Transmission through the semi-transparent plane also results in empty space transmission:

$$\hat{T}(S, C, P)Q(S) = T(C)\hat{T}(S, P)Q(S). \tag{23}$$

Now, the source strength equals that of the source at S times, the transmission coefficient of the panel $T(C)$ defined at the point C where the panel is pierced by the direct path from S to P.

The operator $\hat{R}(S, A, P)$ describes reflection:

$$\hat{R}(S, A, P)Q(S) = R(A)\hat{T}(S', P)Q(S). \tag{24}$$

Its action results in transmission from the point source at S' to the observation point at P. The source at S' is the mirror image of the real source at S with respect to the plane. The strength of the source at S' equals that of the source at S, its image times the reflection coefficient $R(A)$ defined at the point A where the panel is pierced by the direct path from S' to P.

As the transmission operator $\hat{T}(S, P)$ (equation (22)) is defined in relation to the (S, P)-distance, the concept of the image observation point can also be used in the description of the reflection. Then

$$\hat{R}(S, A, P)Q(S) = R(A)\hat{T}(S, P')Q(S), \tag{25}$$

where P' is the mirror image of the real observation point at P with respect to the plane.

The operator describing diffraction at a wedge (edge),

$$\hat{D}(S, E, P)Q(S) = D(v; S, P)\hat{T}(S, P)Q(S), \tag{26}$$

is proportional to the undisturbed wave (equation (22)) by the coefficient $D(v; S, P)$. The point E is the active point at the wedge (edge): e.g., the point through which passes the

shortest path from the source at S to the observation point at P (Fermat's principle). The coefficient $D(v; S, P)$ is a function of the kind of wedge, described by the parameter v, and the source and the observation point positions in relation to the wedge. The parameter v gives the angle $v\pi = 2\pi - 2\Omega$, being the difference of the outer space angle of the wedge and the inner angle 2Ω. The source $S(\rho_0, \varphi_0, z_0)$ and the observation point $P(\rho, \varphi, z)$ positions are given in the co-ordinate system with a z-axis identical with the wedge (edge).

As transmission does not change the radiating source position, only appearance of a reflection in the chain of interactions affects the diffraction coefficient. When reflection occurs before diffraction then, in the diffraction coefficient, there appears an image source of appropriate order, describing the wave history before diffraction. Reflection after diffraction results in the appearance of an appropriate image observation point, describing the wave history after diffraction.

In the model presented, all three kinds of interactions are linear in relation to the undisturbed wave due to the appropriate source at the appropriate observation point. The proportional coefficients are transmission, reflection and diffraction coefficients (equations (22–26)). The transmission and reflection coefficients are regarded as panel acoustical parameters. The reflection process specifics require determination of the image-source position S' or the image observation point P'. The specifics of diffraction require calculation of diffraction coefficient, defined by the source and the observation point position in relation to the wedge.

Since the acoustical wave can reach the observation point by different chains of the three kinds of interactions with panels composing obstacles, for the system containing N panels, and interactions up to the $\mathscr{K}$-order, the acoustical pressure at the observation point is

$$p(S, P) = \sum_{\ell=1}^{\mathscr{K}} \sum_{i=1}^{I(N,\ell)} \hat{\Pi}^i_\ell, (n)^* \ldots {}^* \hat{\Pi}^i_1(n) Q(S)$$

$$= \sum_{\ell=1}^{\mathscr{K}} \sum_{i=1}^{I(N,\ell)} \prod_{\ell'=1}^{\ell} \hat{\Pi}^i_k, (n) Q(S). \tag{27}$$

The i-sequence of the set of operators $[\hat{\Pi}^i_\ell(n), \ldots, \hat{\Pi}^i_1(n)]$, describing the i-path, is one of the possible combinations of $3N$ elements of the set of transmission, reflection and diffraction operators $\{\hat{\Pi}(n)\}$, taken ℓ at a time.

The interaction with the n-panel is given by

$$\hat{\Pi}(n) = \begin{cases} \hat{T}(S^{(p)}, C_n, P^{(r)}) = T(C_n)\hat{T}(S^{(p)}, P^{(r)}), \\ \hat{R}(S^{(p)}, A_n, P^{(r)}) = R(A_n)\hat{T}(S^{(p,n)}, P^{(r)}) = R(A_n)\hat{T}(S^{(p)}, P^{(n,r)}) \\ \hat{D}(S^{(p)}, E_{m(n)}, P^{(r)}) = D(v; S^{(p)}[m(n)], P^{(r)}[m(n)])\hat{T}(S^{(P)}, P^{(r)}) \end{cases}, \tag{28}$$

where the suorce at $S^{(p)}$ and the point $P^{(r)}$ describe the wave history before and after interaction with the n-panel, respectively. The source at $S^{(p,n)}$ is the mirror image of the source at $S^{(p)}$ with respect to the n-panel. The point $P^{(n,r)}$ is the mirror image of the source $P^{(r)}$ with respect to the n-panel. For each diffraction process, occurring at the $m(n)$-wedge of the n-panel, the source at $S^{(p)}$ and observation point $P^{(r)}$ positions are given in the different local co-ordinates system with z-axis identical with the $m(n)$-wedge.

2.3. INTERACTION WITH PANELS

The acoustical pressure of the wave which suffers interaction with the n-panel is written in the form containing all the possible components of the total field [4, 22, 30–33]:

$$p_n(S, P) = \left[\eta(C_n) + (1 - T(n)) \sum_{m=1}^{M} \eta(S, E_m, P)\right] \hat{T}(S, P) Q(S)$$

$$+ \left[\eta(A_n) + R(n) \sum_{m=1}^{M} \eta(S^{(n)} E_m, P)\right] \hat{T}(S^{(n)}, P) Q(S). \tag{29}$$

The terms in the first square brackets describe the wave transmitted through the plane of the n-panel; it depends on the direct wave and the wave transmitted through the n-panel via the transmission coefficient $T(n)$. They are accompanied by diffraction waves connected with the real source S. The factor $\eta(C_n)$ makes a choice between the direct and transmitted waves:

$$\eta(C_n) = \begin{Bmatrix} T(n), & C_n \in (n)\text{-panel} \\ 1, & C_n \notin \text{-panel} \end{Bmatrix}, \tag{30}$$

where C_n is the transmission point at the plane of the n-panel.

The terms in the second square brackets describe the wave reflected from the n-panel of reflection coefficient $R(n)$, accompanied by the diffraction waves connected with the image source $S^{(n)}$. The factor $\eta(A_n)$ gives the regions where the reflection wave exists:

$$\eta(A_n) = \begin{Bmatrix} R(n), & A_n \in (n)\text{-panel} \\ 0, & A_n \notin \text{-panel} \end{Bmatrix}. \tag{31}$$

Here A_n is the reflection point at the plane of the n-panel.

The diffraction terms in equation (29) can be expressed in the same way regardless of whether they are connected with the real or the image source when the appropriate co-ordinates describing the source position are taken. Thus, for the source at S the factor $\eta(S, E_m, P)$ describing diffraction at the m-edge (wedge) is

$$\eta(S, E_m, P) = \begin{Bmatrix} D[v; S(m), P(m)] & E_m \in (m)\text{-edge(wedge)} \\ 0, & E_m \notin (m)\text{-edge(wedge)} \end{Bmatrix}, \tag{32}$$

$$D[v; S(m), P(m)] = P(\varphi_{0m}, \varphi_m, v) V^c(R, R_{em}, \rho_m) D^{s(c)}(R, \rho_{0m}, \rho_m). \tag{33}$$

The position of the active point E_m at the m-edge (wedge) determines, whether the m-edge (wedge) generates the diffraction wave or does not. This is according to the Rubinowicz theory [39] that only the vicinity of the point E_m participates effectively in radiation of the cylindrical wave resulting from diffraction at the edge (wedge). The same comes from the McDonald solution [4] when the steepest descent method is applied.

In equation (33), the parameter v determines the outer space $v\pi = 2\pi - 2\Omega$ around the m-wedge of the inner angle 2Ω. For a single panel playing a role of screen $v = 2$; for a right angle wedge of a building $v = 3/2$. All the factors are expressed for the source

$S(\rho_{0m}, \varphi_{0m}, z_{0m})$ and the observation point $P(\rho_m, \varphi_m, z_m)$ positions given in the co-ordinate system with the m-edge (wedge) as the z-axis. The factor

$$P(\varphi_m, \varphi_{m0}, \nu) = \frac{1}{\nu} \sin(\pi/\nu) \frac{1}{\cos(\pi/\nu) - \cos\{(\varphi_m - \varphi_{0m})/\nu\}} \tag{34}$$

represents the directional patterns of the cylindrical wave emitted by the edge (wedge),

$$V^c(R, R_{em}, \rho_m) = \frac{\exp\{\mathrm{i}[k(R_{em} - R) + \pi/4]\}}{\sqrt{2\pi k \rho_m}}, \tag{35}$$

where

$$R = \sqrt{R_{em}^2 - 4\rho_{0m}\rho_m \cos^2[(\varphi_m - \varphi_{0m})/2]}, \qquad R_{em} = \sqrt{(\rho_{0m} + \rho_m)^2 + (z_m + z_{0m})^2}. \tag{36, 37}$$

When the spherical wave reaches the edge (wedge), as it does in the case of a wave emitted by the point source, the deformation factor is

$$D^s(R, \rho_{0m}, \rho_m) = kR/\sqrt{kR_{em}k\rho_{0m}}. \tag{38}$$

When the wave reaching the edge (wedge) is of the cylindrical type as it is during diffraction of order higher than one, then

$$D^c(R, \rho_m) = \sqrt{kR/k\rho_{0m}}. \tag{39}$$

When the m-edge (wedge) is an active one (equation (32)), the diffraction can be interpreted as radiation of the source at the m-edge (wedge) because it represents transmission of the cylindrical wave $V^c(R, R_{em}, \rho_m)$ (equation (35)) born at the m-edge (wedge). The source is the secondary source of the strength given by $[D^{s(c)}(R, \rho_{0m}, \rho_m)\hat{T}(S, P)Q(S)]$ and of the directional patterns given by $P(\varphi_{0m}, \varphi_m, \nu)$.

The geometrical part of the field in equation (29)

$$\begin{aligned} p_n^g(S, P) &= p^t(S, C_n, P) + p^r(S, A_n, P) \\ &= \eta(C_n)T(S, P)Q(S) + \eta(A_n)T(S^{(n)}, P)Q(S) \\ &= \left\{ \begin{matrix} \hat{T}(S, P)Q(S), \; C_n \notin (n)\text{-panel}, \\ \hat{T}(S, C_n, P)Q(S), \; C_n \in (n)\text{-panel}, \end{matrix} \right\} + \hat{R}(S, A_n, P)Q(S), \end{aligned} \tag{40}$$

contains the two types of transmitted waves: the direct wave or the wave transmitted through the n-panel, and the wave reflected from the n-panel. All the waves are expressed by the action of the appropriate operators on the source $Q(S)$.

The diffraction part of the field in equation (29) is

$$\begin{aligned} p_n^d(S, P) &= \sum_{m=1}^{M} p^d(S, E_m, P) + \sum_{m=1}^{M} p^d(S, C_n, E_m, P) + \sum_{m=1}^{M} p^d(S, A_n, E_m, P) \\ &= (1 - T(n)) \sum_{m=1}^{M} \eta(S, E_m P)\eta(C_n)\hat{T}(S, P)Q(S) \\ &\quad + R(n) \sum_{m=1}^{M} \eta(S^{(n)}, E_m, P)\hat{T}(S^{(n)}, P)Q(S) \\ &= (1 - T(n)) \sum_{m=1}^{M} \hat{D}(S, E_m, P)Q(S) + R(n) \sum_{m=1}^{M} \hat{D}(S^{(n)}, E_m, P)Q(S). \end{aligned} \tag{41}$$

The diffraction part of the field is formed by the three kinds of diffraction waves, each of them connected with the source of the geometrical wave: direct, transmitted through the n-panel and reflected from it. Simultaneously, the diffracted waves are expressed by the appropriate diffraction operators as independent processes at wedges (edges) of the n-panel.

As has been shown above, from the point of view of wave interaction, the urban system can be regarded as a composition of N panels and M wedges (some of them may be edges). The wave is transmitted through the panels and reflected from them, and by wedges it is diffracted, thus,

$$\left.\begin{array}{l}\hat{T}(\ldots, C_n, \ldots)\\ \hat{R}(\ldots, A_n, \ldots)\end{array}\right\} = \hat{I\!I}(n) \left.\begin{array}{l}\\ \\ \hat{D}(\ldots, E_m, \ldots) = \hat{I\!I}(m)\end{array}\right\} = \hat{I\!I}(\mu). \tag{42}$$

The set of operators $\{\hat{I\!I}(\mu)\}$, describing all the possible interactions, contains $2N + M$ elements. This means that the number of operators is equal to the number of elements of the urban system with which a wave can independently interact. The wave i-path, on which ℓ interactions are assumed, is described by the i-sequence of the operators $[\hat{I\!I}^i_\ell(\mu), \ldots, \hat{I\!I}^i_1(\mu)]$. It is an ordered combination of $2N + M$ operators, taken ℓ at a time. In the i-sequence the same operator can appear more than once. In combinatorics, such an i-sequence is called the ℓ-tuple of the $2N + M$ elements of the set $\{\hat{I\!I}(\mu)\}$ with repetitions.

Now, for the number of interactions up to the $\mathscr{K}$-order, the total field (equation (27)) can be rewritten as a sum of the geometrical and diffraction parts:

$$p(S, P) = p^g(S, P) + p^d(S, P), \tag{43}$$

$$p^g(S, P) = \sum_{\ell=1}^{\mathscr{K}} \sum_{i=1}^{I(N,\ell)} \prod_{\ell'=1}^{\ell} \hat{I\!I}^i_{\ell'}, (n)Q(S)$$

$$= \sum_{\ell=1}^{\mathscr{K}} \sum_{i=1}^{I(N,\ell)} p_i(S, P; \ell), \tag{44}$$

$$p^d(S, P) = \sum_{\ell=1}^{\mathscr{K}} \sum_{i=1}^{I(N,M,\ell)} \prod_{\ell'=1}^{\ell} \hat{I\!I}^i_{\ell'}, (\mu)Q(S)$$

$$= \sum_{\ell=1}^{\mathscr{K}} \sum_{i'=1}^{I(N,M,\ell)} p_{i'}, (S, P; \ell). \tag{45}$$

The geometrical part of the field $p^g(S, P)$ (equation (44)) is composed of the terms containing only transmissions and reflections. The diffraction part of the field $p^d(S, P)$ (equation (45)), apart from transmission and reflections contains the terms in which diffraction appears, at least once.

The different sequence of operators, acting on the source $Q(S)$, gives different terms (waves) in equations (44) and (45) as each term describes a different wave path determined by the sequence of points where the interactions take place. The product of operators is non-commutative because the positions of transmission, and reflection points on panels, and the active points at wedge (edges) are determined by the position of the point where the source of the wave is for the process, and the position of the point at which the next interaction takes place [30].

In equation (44), as one of the first order geometrical terms, the term $\kappa = 1$ appears, which represents the direct wave (equation (23)). Other first order geometrical terms result as a consequence of the single processes of transmission through the panels and reflection from them. The second order geometrical terms ($\kappa = 2$) result from action of any combination of the pair of operators $\hat{T}\hat{T}$, $\hat{R}\hat{R}$, $\hat{T}\hat{R}$, $\hat{R}\hat{T}$.

The first order diffraction terms (equation (45)) result from diffraction of the direct wave. When, before diffraction, the wave is transmitted or reflected then the second order terms ($\kappa = 2$) appear since they result from action of the two operators $\hat{D}\hat{T}$ or $\hat{D}\hat{R}$. When a wave diffracted at edges (wedges), before reaching the observation point, is subjected to transmission or reflection then a second order term, being a product of operators $\hat{T}\hat{D}$ or $\hat{R}\hat{D}$, appears.

The third order terms $\hat{D}\hat{R}\hat{D}$ appear, e.g., when the wave, due to the source at S, before diffraction at the m-wedge, is first reflected from the p-panel and after diffraction from the r-panel:

$$\begin{aligned} p_i(S, P; \kappa = 3) &= p^d[S, A(i)_p, E(i)_m, A(i)_r, P] \\ &= \hat{R}[E(i)_m, A(i)_r, P][\hat{D}[S, E(i)_m, P](\hat{R}[S, A(i)_p, E(i)_m]Q(S))] \\ &= \eta(A_p)\eta(A_r)\eta(S^{(p)}, E_m, P^{(r)})\hat{T}(S^{(p)}, P^{(r)})Q(S) \\ &= \eta(A_p)\eta(A_r)\eta(S^{(p)}, E_m, P^{(r)})\frac{\exp[\mathrm{i}kR(S^{(p)}, P^{(r)})]}{R(S^{(p)}, P^{(r)})}. \end{aligned} \tag{46}$$

As can be seen from the above, the higher order terms in equations (46) and (45) result when one of the operators $\hat{T}$, $\hat{R}$, $\hat{D}$ acts on a term of lower order which plays the role of an undisturbed wave for the process (equations (22–26)). Since all interactions are linear in relation to the undisturbed wave, eventually, as a result one obtains the product of transmission, reflection and diffraction coefficients, which appears in front of the transmission operator from the appropriate source (real or image) to the observation point (real or image), which provides the undisturbed wave.

3. SIMULATION MODEL

The above description of the highway model (section 2.1) and the propagation model (sections 2.2, 2.3) describing wave interactions with buildings are enough to construct the noise environmental model in an urban area (equation (1)), and next, the simulation program.

The prepared PROP3 simulation program allows one to calculate the sound equivalent level at points of interest:

$$\begin{aligned} L_{eq}(\mathrm{dB(A)}) = \hat{\Pi}_0\left(10\log; p_0^2; \int \mathrm{d}\omega, \Delta L_A(\omega)\right) \\ * \hat{\Pi}(N, \{\mathbf{R}(n)\}, \{R(n)\}, \{T(n)\}, \mathscr{K}, \mathbf{R}(P))Q_A(\ldots). \end{aligned} \tag{47}$$

The propagation model $\hat{\Pi}(\,)$ contains the following as the parameters: N, number of panels; $\{\mathbf{R}\}$, set of vectors describing geometry of panels; $\{R(n)\}$, set of reflection coefficients of panels; $\{T(n)\}$, set of transmission coefficients of panels; $\mathscr{K}$, upper order of interaction; $\mathbf{R}(P)$, observation point position.

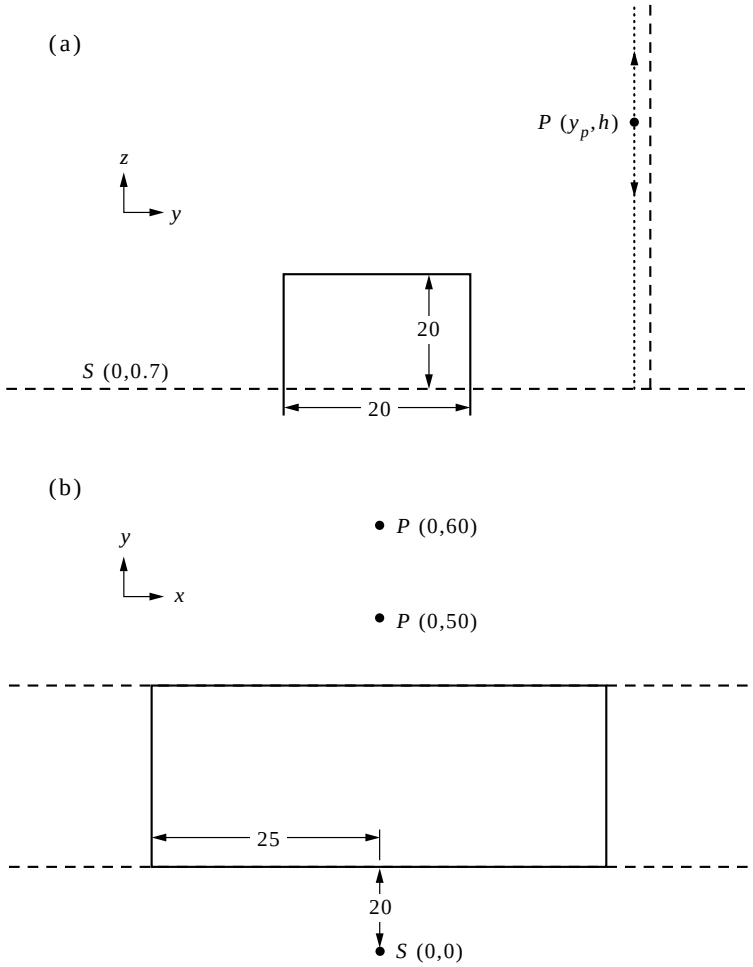

Figure 3. The stationary source and observation points' positions during investigation of the single building shielding efficiency: (a) vertical projection; (b) horizontal projection (dimensions in metres).

The two applied options of the source model $Q_A(\,)$ for a stationary source and a highway,

$$Q_A(\ldots) = \begin{Bmatrix} Q(\mathbf{R}(S),\, w_{rA}(S, f_w),\, SPL(1,1)) \\ Q(N,\, v,\, J,\, \{\mathbf{R}_j\},\, \Delta x_E,\, w_{rA}(f_w),\, SPL(1,1)) \end{Bmatrix}, \tag{48}$$

contains the following as parameters: N, total mean flow rate (vehicles/h); v, average vehicle speed (m/h); J, number of lanes; $\mathbf{R}(S)$, position of source S; Δx, average vehicle spacing; $\{\mathbf{R}_j\}$, set of vectors describing geometry of lanes: Δx_E, summation step; $w_{rA}(S, f_w)$, relative, A-weighted power level of spectrum of S source; $w_{rA}(f_w)$, relative, A-weighted power level of spectrum of traffic noise: $SPL(1, 1)$, sound pressure level in 1 kHz octave-band, at a distance of 1 m from the equivalent point source.

The simulation program PROP3 gives a quantitative answer to how the sound equivalent level changes as a result of the changes in the source parameters (equation (48)) and the urban system parameters (equation (47)). In an urban system, sometimes, a change

TABLE 1

The single building investigation (*see Figure* 3)

Case No.	Number of sources	Δx_E (m)	Left-side length (m)	Right-side length (m)	$R(n=1)$	$R(n=7)$	y_p
1	1	—	∞	∞	0	0	60
2	1	—	25	∞	0	0	60
3	1	—	25	25	0	0	60
4	1	—	25	25	0·9	0	60
5	1	—	25	25	0·9	0·9	60
6	5	80	25	25	0·9	0	60
7	7	80	25	25	0·9	0	50
8	13	40	25	25	0·9	0	60

Δx_E is the distance between sources' positions on the lane; $R(n=1)$ is the reflection coefficient of the ground; $R(n=7)$ is the reflection coefficient of the plane behind the observation points; y_p is the observation point co-ordinate.

of the reflection coefficients of panels (walls, ground surface) is possible. However, the decisive factors are the mutual arrangements of buildings, their dimensions, and their locations in relation to the source (a highway) position. They could be arbitrary, according to the designer architectural fantasy. The PROP3 can give an answer to the question of what value of the sound equivalent level will be at the point of interest, especially on building facades [31], for any imagined arrangement of buildings.

The accuracy of the sound level calculation (equation (47)) is affected by the simulation model accuracy, and the adequacy of the simulation model to the real conditions.

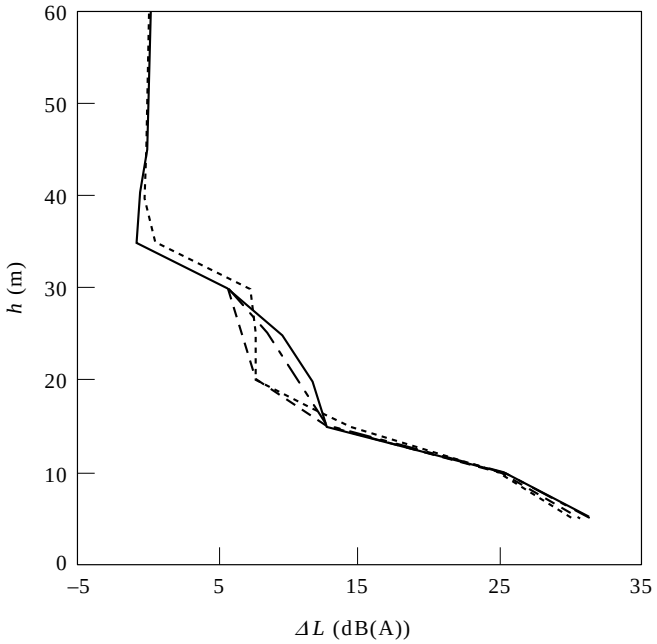

Figure 4. The stationary source shielding efficiency by the single building (see Figure 3, Table 1): (1) ——, of unlimited length, in free space; (2) – – –, of one-side unlimited length, in free space; (3) ———, of limited length, in free space; (4) ——, of limited length, in the semi-space with the ground.

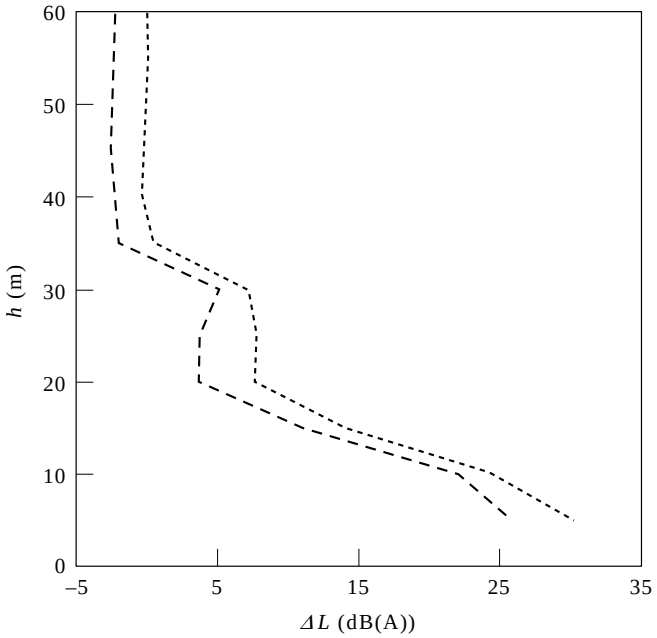

Figure 5. The single building shielding efficiency for the stationary source (see Figure 3, Table 1): (4) ——, without the additional plane behind the observation points; (5) ———, with the plane.

Both the source model and the propagation model, are constructed for far field conditions. Upon taking into account the A-weighted noise spectra met in urban area, it may be stated that distances from a source to the place of the first interaction, and between subsequent interactions are of the order of a few wavelengths of the dominant component. Thus, the simulation model is the proper one.

The sound equivalent level from a highway is related to the sound exposure (acoustical energy) due to an individual vehicle drive-by. This energy is not calculated as an integral along the path travelled but as a sum of energies at the sequence of discrete positions along the path. At each discrete position, a wave is emitted by an equivalent point source, and the acoustical pressure at the observation point is the sum over all the possible wave paths, with phases included. The assumption that the wave front is locally flat allows one to calculate the energy for each discrete source position as proportional to the mean square pressure. Next, the energies of all the discrete positions are summed up to obtain the sound exposure. Thus, the source model made up of point sources of a given power spectrum with a directivity characteristic (when it is needed) is adequate, and its accuracy depends on the accuracy with which the parameters are measured and the value of the discretization step.

In the propagation model, the description of elementary interactions includes transmission, reflection, diffraction. Its accuracy depends on the assumed upper order of interactions $\mathscr{K}$, which can be chosen in a step-by-step procedure. However, the geometry of an urban system is simplified and the real obstacles are replaced by shoe-boxes or plane panels. Also, all the effects connected with inhomogeneity of the propagation medium and changeable meteorological conditions are omitted. Because of these two reasons the adequacy of this description is still an open question.

There are attempts to describe sound propagation in an urban area as a diffusion process through statistically scattered obstacles (buildings) [50–53]. In this case the urban system

transfer function (propagation model) depends only on two parameters: average building density, and average attenuation factor related to interaction with obstacle. For some purposes this approach can be suitable. Generally, it is difficult to find in an urban area conditions close to the conditions met in gas mechanics, where the diffusion model works well.

When someone is interested in noise fluctuations, in noise indices L_1, L_{10}, L_{50}, L_{90} [54–65], the distribution function has to be introduced into the source model, for vehicle parameters such as vehicle position, number of vehicles, vehicle acoustical power, vehicle flow rate fluctuations. This was done, e.g., in the case when the distribution function was applied to vehicle position on a highway with the propagation model based on the image sources method [66, 67].

To sum up, the simulation model accuracy depends on the modelling adequacy and the accuracy with which the parameters are measured. Some of these parameters are not easily obtained. However, the absolute value of the sound equivalent level L_{eq} is not always required. More often the change in the sound equivalent level L_{eq} caused by a change in the source and/or propagation parameters (equations (47, 48)) is sought. When the assumption is made that the phenomena omitted and simplifications influence the differently analysed situation in the same way, the information provided by the simulation model can be regarded as reliable.

3.1. SHIELDING EFFICIENCY CALCULATION

By use of the simulation model (equations (47, 48)), the shielding efficiency can be defined for the highway segment of J lanes parallel to the x-axis, with the total average flow rate N (vehicles/h), and the average vehicle speed v (m/h). It is the difference between

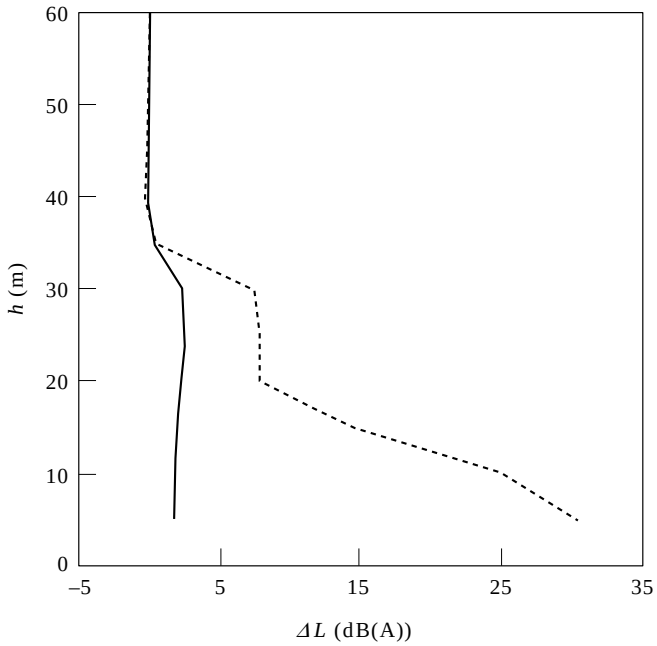

Figure 6. The shielding efficiency of the single building (see Figure 3, Table 1): (4) ———, for the stationary source; (6) ——, for the moving source.

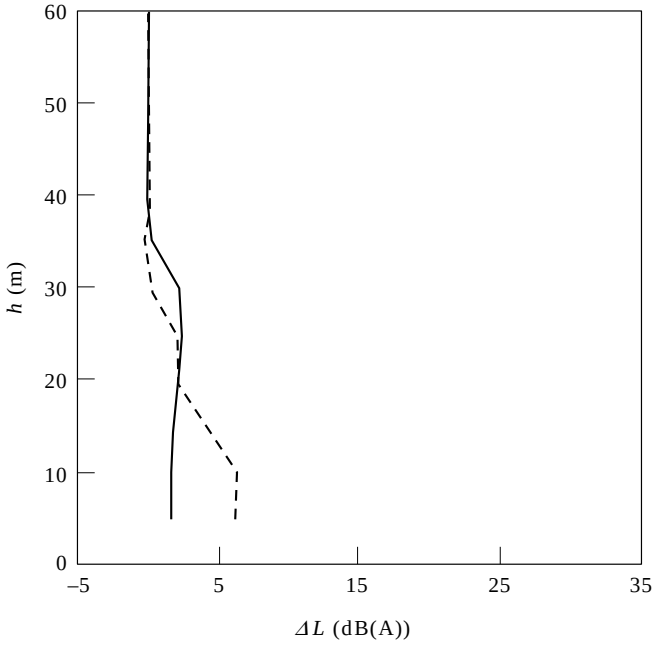

Figure 7. The shielding efficiency of the single building for the moving source at two distances behind the building (see Figure 3, Table 1): (6) ——, 20 m; (7) – – –, 10 m.

the sound equivalent level in the half-space limited by the ground surface ($N = 1$), and the sound equivalent level in the actual urban system:

$$\begin{aligned}\Delta L_{eq}(T = 1\text{h})(\text{dB(A)}) &= L_{eq}(N = 1, \mathbf{R}(n = 1),\\ &R(n = 1), \mathbf{R}(P); \{\mathbf{R}(S_u)\}, w_{rA}(f_w), U(\Delta x_E))\\ &\quad - L_{eq}(N, \{\mathbf{R}(n)\}, \{R(n)\}, \{T(n)\}, \mathscr{K}, \mathbf{R}(P); \{\mathbf{R}(S_u)\}, w_{rA}(f_w), U(\Delta x_E))\\ &= 10 \log \sum_{w=1}^{W} 10^{0{\cdot}1 w_{rA}(f_w)} \frac{1}{S_w} \sum_{s=1}^{S_w} \sum_{u=1}^{U(\Delta x_E)} \left| \sum_{i=1}^{I(N=1)} p_i(S_u, P, f_{ws}) \right|^2\\ &\quad - 10 \log \sum_{w=1}^{W} 10^{0{\cdot}1 w_{rA}(f_w)} \frac{1}{S_w} \sum_{s=1}^{S_w} \sum_{u=1}^{U(\Delta x_E)} \left| \sum_{\ell=1}^{\mathscr{K}} \left[\sum_{i=1}^{I(N,\ell)} p_i(S_u, P, f_{ws}; \ell) \right.\right.\\ &\quad \left.\left. + \sum_{i'=1}^{I(N,M,\ell)} p_{i'}(S_u, P, f_{ws}; \ell) \right] \right|^2. \end{aligned} \tag{49}$$

The shielding efficiency of a single building and in the three differently arranged systems of five buildings have been investigated. As a noise source, an individual vehicle is represented by the equivalent point source, the two source models are assumed: the stationary equivalent source and the equivalent source which moves along one of the highway lanes. Insertion of the second source model into the shielding efficiency expression (equation (49)) instantly gives the shielding efficiency for the one-lane highway. This is due to the fact that the average spacing between successive vehicles on the lane Δx (equation (7)), present in the sound level expression (equation (10)), disappears in the shielding

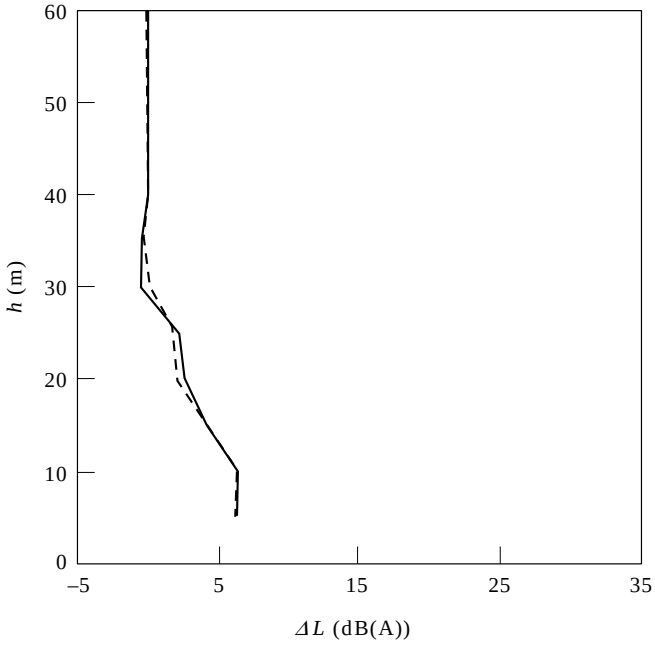

Figure 8. The single building shielding efficiency for the moving source with the summation step (see equation (49)): (7) ——, $\Delta x_E = 80$ m; (8) ——, $\Delta x_E = 40$ m.

efficiency expression ΔL_{eq} (equation (49)), which makes it independent of the rate flow of vehicles on the lane and their average speed.

For the given parameters of the highway and the urban system, the shielding efficiency depends on the summation step Δx_E through the number of point sources $U(\Delta x_E)$ (equation (12)) representing vehicles moving along J lanes of the highway segment and through the positions of S_u sources (equations (13–16)).

TABLE 2

The system of five buildings investigation (*see Figures* 9–11)

Case No.	Number of sources	(x_1, x_2) (m)	Δx_E (m)	α (deg)	(x_{p1}, x_{p2}) (m)	y_p (m)
10	1	(0, 0)	—	90	(−60, 160)	80
11	1	(0, 0)	—	0	(−90, 180)	50
12	1	(0, 0)	—	45	(−60, 200)	80
13	10	(−320, 400)	80	90	(−60, 160)	80
14	9	(−240, 400)	80	0	(−90, 180)	50
15	10	(−320, 400)	80	45	(−60, 200)	80
16	19	(−320, 400)	40	90	(−60, 160)	80
17	17	(−240, 400)	40	0	(−90, 180)	50
18	19	(−320, 400)	40	45	(−60, 200)	80
19	9	(−280, 360)	80	0	(−90, 180)	50
20	10	(−340, 380)	80	45	(−60, 200)	80

x_1, x_2 are the ends of the highway lane; Δx_E is the distance between sources' positions on the lane; α is the angle formed by the longer building side with x-axis, at the building corner nearest to the lane; x_{p1}, x_{p2} are the ends of the line of observation points; y_p is the observation point co-ordinate.

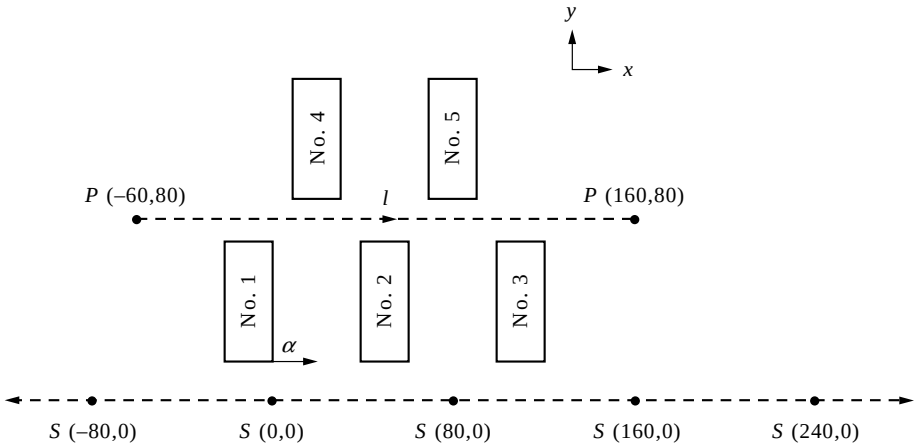

Figure 9. The urban system of five buildings located perpendicularly to the highway lane (dimensions in metres).

When the number of the sources grows, i.e., when Δx_E decreases, the sound level in the empty half-space (equation (49)) approaches the value characteristic for the line source of limited length. In the half-space with buildings, the number of sources and their exact positions on the lanes are the decisive factors in calculation of the sound level (equation (49)) as they determine the possible paths of reaching the observation point. In this case the influence of the Δx_E value is less predictable but for some small enough values of Δx_E the shielding efficiency is expected to be independent of it.

In the urban system analysed, the most favorable conditions for sound propagation through the openings in the first row of buildings to the observation point, lying behind them, create the situation which is the nearest to calculation of the integral along the source path. The required conditions could be obtained not only by decrease of the value of Δx_E (which enlarges the number of sources) but also by finding the appropriate positions of sources with relatively large values of Δx_E. The choice of optimal number of sources at the proper positions saves computation time. For example, for the five buildings system analysed and interaction up to the third order, calculation on PC 386/40 MHz, for one source and one observation point, took about 10 min. Therefore, the effect on the shielding efficiency due to the value of Δx_E and S_u sources positions has been tested.

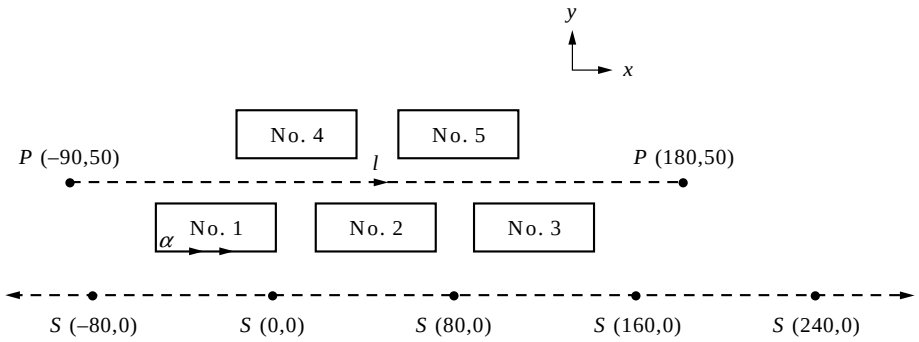

Figure 10. The urban system of five buildings located parallel to the highway lane (dimensions in metres).

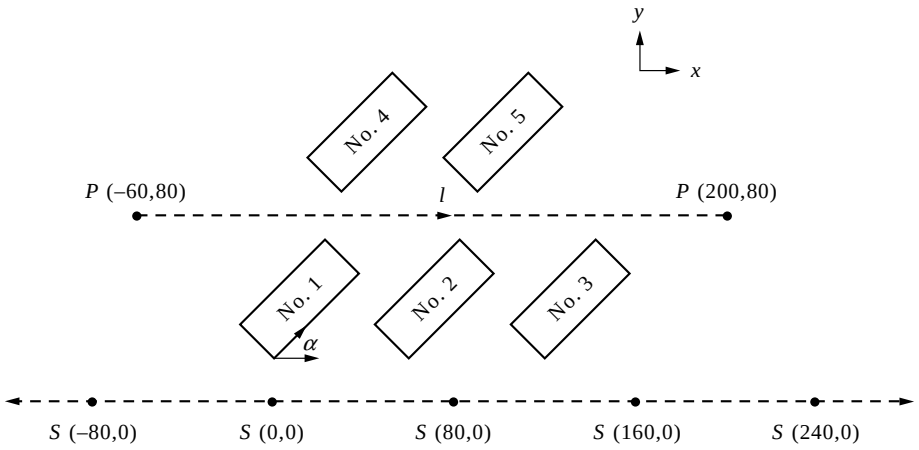

Figure 11. The urban system of five buildings inclined to the highway lane (dimensions in metres).

3.1.1. *Shielding efficiency of a single building*

The shielding efficiency of the single building 12 m high and 20 m wide (see Figure 3) has been investigated. The assumed stationary source is at the central position in front of the building at a distance of 20 m from the building facade. The observation points are on the vertical line at the central position, 20 or 10 m behind the building.

The influence of the building's limited length on its shielding efficiency, presence of the ground and the additional plane behind the observation points (representing a facade of a protected building) has been investigated for the stationary source (see Table 1, cases 1–5). The moving source modelled by the sources distributed with the step Δx_E along the parallel to the building, at a distance of 20 m in front of the building, has also been investigated (see Table 1, cases 6–8), where the stationary source becomes one of the sources on the lane.

The shielding efficiency of the building, treated as an acoustical screen for the single source, is presented in Figures 4 and 5. In Figure 4, it is shown how the building shielding efficency changes when the building length becomes limited. The one-side limitation, in addition to the wave doubly diffracted at the building's upper wedges (curve (1)), introduces the wave being doubly diffracted at the building side wedges of one of the building's ends (curve (2)). In the case of a two-side limitation, two additional waves appear, being doubly diffracted at the two ends of the building (curve (3)). Introduction of the ground, of reflection coefficient 0·9, causes the appearance, for each already existing wave, of its counterparts reflected from the ground in front of the building, before diffraction, and behind the building, after diffraction at its wedges (curve (4)).

In Figure 5 the influence of the additional plane behind the observation points is presented (curve (5)). The situation is adequate when the building acts as a protector for the second one, behind it. The existence of two parallel surfaces: the rear wall of the first building and the protected facade of the second one causes, reflections that diminish the shielding efficiency in relation to the situation when the additional plane is absent (curve (4)).

Figure 6 presents the shielding efficiency of the building for the stationary source at the central position (curve (4)) and for the moving source (curve (6)). The moving source is effectively shielded only at its position just in front of the building; at other positions it emits direct waves reaching the observation points. In Figure 7 the efficiency for the

moving source, observed at distances of 10 m (curve (6)) and 20 m (curve (7)) behind the building, is presented. In each case the end points on the highway lane are chosen according to equation (8). It is seen that a noticeable shielding efficiency of the single building for the moving source can be expected for the points behind the building at distances smaller than 20 m.

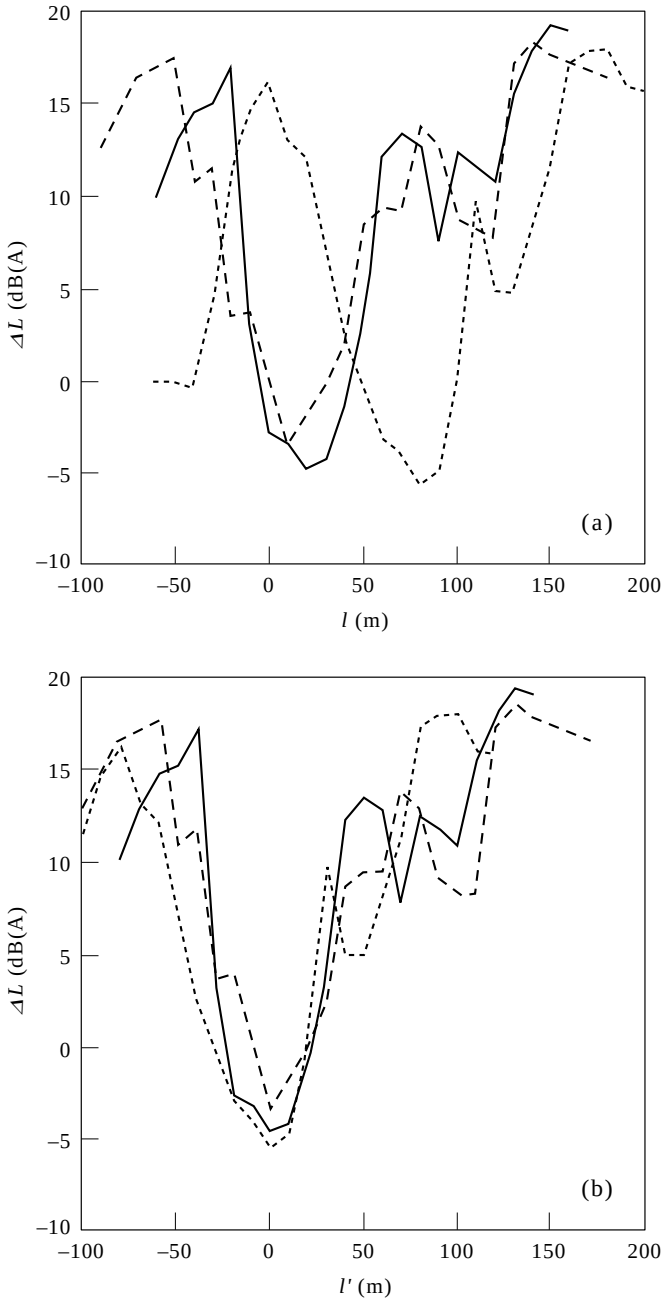

Figure 12. The shielding efficiency for the stationary source in the urban system of five buildings (see Table 2) (a): (10) ——, perpendicular (see Figure 9); (11) — — —, parallel (see Figure 10); (12) – – –, inclined (see Figure 11); (b) the same as (a) but with shifted l-axis: (10) $l' = l + 20$; (11) $l' = l + 10$; (12) $l' = l = 80$.

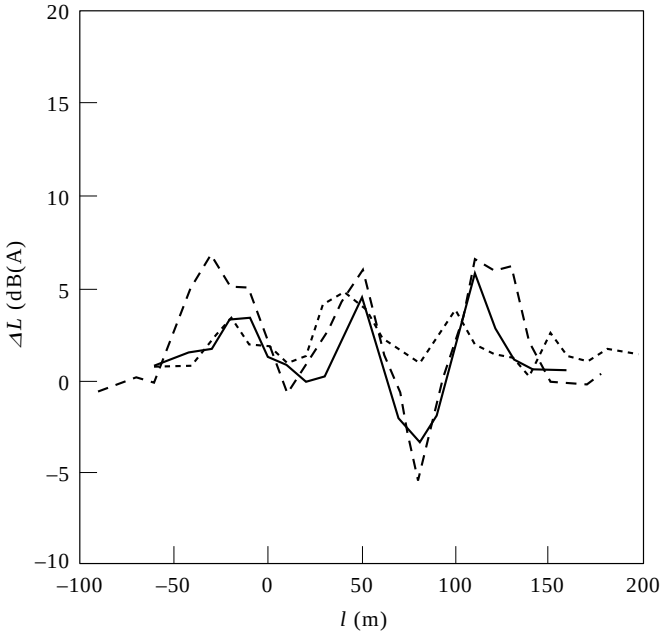

Figure 13. The shielding efficiency for the moving source in the urban system of five buildings (see Table 2): (13) ——, perpendicular (see Figure 9); (14) ———, parallel (see Figure 10); (15) – – –, inclined (see Figure 11).

Figure 8 presents the influence of the Δx_E step in the discrete summation (equations (10–16)) on the shielding efficiency. To investigate these effects two values of $\Delta x_E = 80$ m (curve (7)), $\Delta x_E = 40$ m (curve (8)) have been taken. The value of $\Delta x_E = 80$ m has been taken arbitrarily as the upper limit for the summation step because of the expression for the sound equivalent level (equation (10)) where for $N_j = 3000$ vehicles/h and $v = 60$ km/h, $\Delta x = 80$ m, and with $\Delta x_E = 80$ m the first term disappears. An assumption of $\Delta x_E = 40$ m has only a small affect on the result. Therefore, in the case of the single building the influence of the Δx_E value is negligible but still it has to be remembered that the influence depends on the urban system geometry; this is discussed in what follows.

3.1.2. *Shielding efficiency of the row of buildings*

The calculation of the shielding efficiency has been performed for an urban system containing five buildings. The single building dimensions are the same as previously $(50 \times 20) \times 12$ m. The reflection coefficients of the ground and buildings' walls are taken real and equal to 0·9. Three different arrangements of the buildings are investigated: perpendicular to the highway (Figure 9); parallel to the highway (Figure 10); inclined to the highway at the angle $\alpha = 45^\circ$ (Figure 11).

The shielding efficiency is calculated for the stationary source at a distance of 20 m from the right corner of building No. 1 and for a moving source (Table 2, cases 10–12). The moving source is modelled by sources distributed along the highway lane parallel to the building system in such a way that the stationary source investigated before is one of the sources on the lane (Table 2, cases 13–15).

The observation points are at the line parallel to the highway, 10 m behind the first row of the buildings, at a height of 1·8 m. The ends of the observation points line are chosen arbitrarily but the ends of the highway lane are calculated according to equation (8) in relation to the end observation points.

In Figure 12, the shielding efficiency in the three differently arranged urban systems are presented for the stationary source $S(0, 0)$ (Figures 9–11) emission. In Figure 12(b) the abscissae are shifted in relation to those in Figure 12(a) to obtain for each curve $l' = 0$ at the centre of the region where the direct wave from the source $S(0, 0)$ arrives. In these regions, for all the three arrangements of buildings, the shielding efficiency is negative. This means that the noise propagated through the system of buildings is amplified.

In Figure 13 the shielding efficiency in the three urban systems of different arrangements are presented for the moving source. For all three arrangements of buildings the shielding efficiency becomes smaller than that for the stationary source and is in the range from -5 to $+5$ dB(A). The negative minima in the curves (13) and (14) have a simple explanation. They appear in the region of existence of the direct wave due to the source $S(0, 0)$ (Figures 9 and 10). For curve (15) there is not so simple an explanation.

In Figures 14 and 16 the shielding efficiency in the given system is presented for the stationary point source and for the moving source for the two values of the summation step $\Delta x_E = 80$, 40 m. Generally, the shielding efficiencies for the moving source become smaller than that for the stationary source in the regions where the direct wave from the stationary source $S(0, 0)$ is well shielded and become larger in the regions where the wave is present.

By taking the two values of the summation step Δx_E it can be seen that the smaller Δx_E is, the smoother is the curve representing the shielding efficiencies. As the shielding efficiency depends on the summation step Δx_E not only through the number of point sources $U(\Delta x_E)$ (equation (12)) representing vehicles moving along a lane, but also through the positions of the S_u sources (equations (13–16)) this effect has been investigated. For the case of the parallel buildings arrangement (Figure 10), by keeping the step value $\Delta x_E = 80$ m and shifting the sources system by 40 m to the left in relation to the case

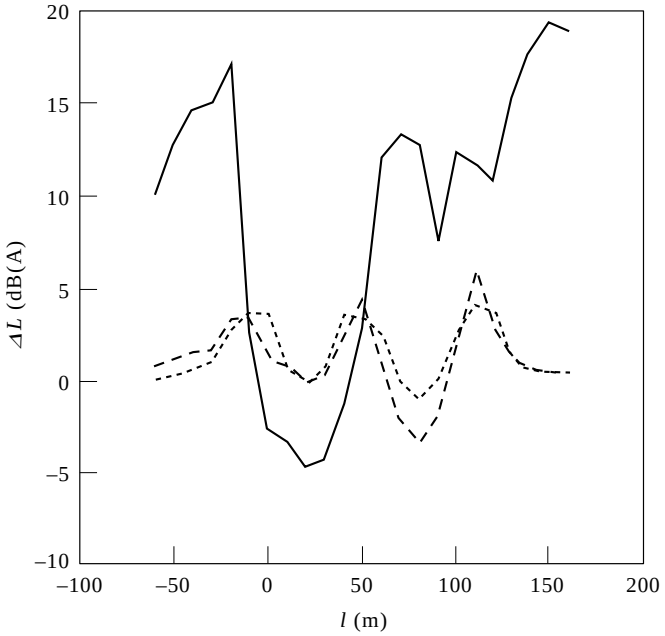

Figure 14. The shielding efficiency in the system of five buildings perpendicular to the highway lane (see Figure 9, Table 2): (10) ——, for stationary source; (13) – – –, for moving source with $\Delta x_E = 80$ m; (16) – – –, for moving source with $\Delta x_E = 40$ m.

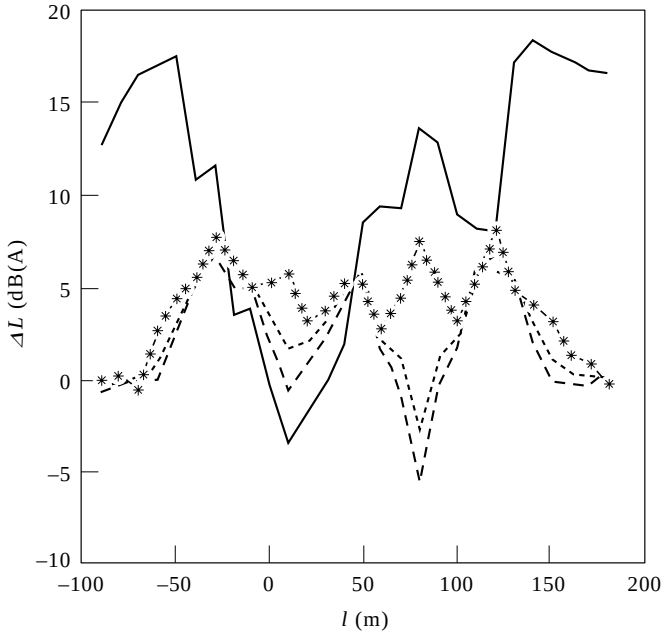

Figure 15. The shielding efficiency in the system of five buildings parallel to the highway lane (see Figure 10, Table 2): (11) ——, for stationary source; (14) ———, for moving source with $\Delta x_E = 80$ m; (17) – – –, for moving source with $\Delta x_E = 40$ m; (19) *—*—*, for moving source with $\Delta x_E = 80$ m and the source system shifted by 40 m in relation to the case of curve (14).

represented by the curve (14) (curve (19) in Figure 15), the full shielding of the direct wave due to the three central sources on the lane $S(-120, 0)$, $S(-40, 0)$, $S(40, 0)$ has been obtained. Owing to this, curve (19) is more similar to curve (11) for the stationary source than curve (14) for which the Δx_E step is the same but the sources' positions are different.

The same effect has been tested for the system of buildings inclined to the highway lane (Figure 11). In Figure 16 for curves (15) and (20) the summation step is the same ($\Delta x_E = 80$ m) but in the case of curve (20) the source system is shifted to the left by 20 m in relation to the case of curve (15). Now, the differences between curves (15) and (20) are negligible.

A general comparison for the three different building arrangements can be done (see Table 3). As a parameter the value of the percentage of openings in the first row of buildings is introduced. It can be seen that the higher the percentage of openings the smaller is the influence of the Δx_E value on the shielding efficiency. The shielding efficiency on the line behind the first row of buildings fluctuates. Its mean value for all three different building arrangements is not large, and ranges between 1 and 2 dB(A).

4. CONCLUSIONS

The PROP3 computer program is a tool for sound level calculation near the facade of a building which is placed in an urban system. In this paper it has been used for calculation of the shielding efficiency of a single building and in an urban system of the five buildings. The shielding efficiency has been calculated for a stationary source and for a source moving along a highway lane.

It is shown how the shielding efficiency of the building changes when the building, first treated as a broad obstacle of a given width, becomes an obstacle of the shoe-box shape

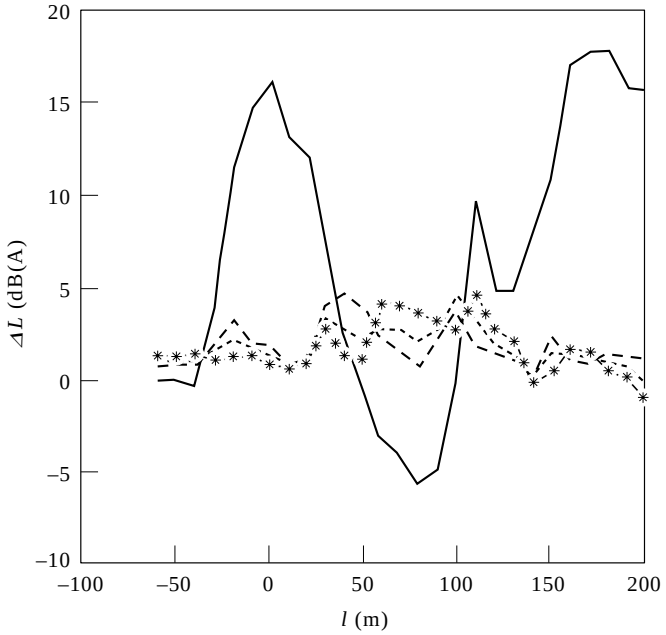

Figure 16. The shielding efficiency in the system of five buildings inclined to the highway lane (see Figure 11, Table 2): (12) ——, for stationary source; (15) — — —, for moving source with $\Delta x_E = 80$ m; (18) – – –, for moving source with $\Delta x_E = 40$ m; (20) ∗—∗—∗, for moving source with $\Delta x_E = 80$ m and the source system shifted by 20 m in relation to the case of curve (15).

placed on the ground, which plays the role of a protector for a facade of another building. During the process the building shielding efficiency decreases.

A drastic decrease of the shielding efficiency is observed when the stationary source is replaced by the moving source. A positive effect could be observed just behind the building.

Next, the shielding efficiency of the first row of buildings, in the system of five differently arranged buildings, has been examined. The collective effect of the first row of buildings has been tested at a line with the observation points behind it, in front of the second row.

TABLE 3

Comparison of shielding efficiency ΔL for the three different building arrangements (see Table 2)

Building arrangement	Case No.	Percentage of openings	Δx_E (m)	ΔL (dB(A))	
				Mean value	Range of change
Perpendicular	13	67	80	1·14	9·25
	16		40	1·43	5·22
Parallel	14	29	80	1·90	12·40
	17		40	2·63	10·41
Inclined	15	72	80	1·82	4·74
	18		40	1·74	4·66

Δx_E is the distance between sources' positions on the lane.

Generally, the mean value of the shielding efficiency for the moving source is very low regardless of the buiding arrangement. The openings in the first row of the buildings provide propagation channels where, because of reflections from the channel walls, noise is amplified. This results in negative shielding efficiency at some points. At other points, as the moving source is represented by a sequence of the sources along a line, only some of these sources can be shielded. Therefore, nowhere does a deep shadow exist. This yields a shielding efficiency value which is relatively small.

Interpreting the results obtained by application of the PROP3 simulation program, the patterns of its construction have been borne in mind (section 3). The values obtained for the sound equivalent level or the shielding efficiency, as it is in the presented examples, are functions of assumed parameters present in the source and propagation model. The upper order of interactions $\mathscr{K}$ on the wave path to the observation point, and the summation step Δx_E of the moving source model are the operational parameters. In all the calculation examples it is assumed $\mathscr{K} = 3$. Special attention has to be paid to the assumed summation step Δx_E. As this step influence is changeable depending on the urban sysem arrangement, there is no general rule how small it has to be, and it should be chosen by inspection.

Generally, as in the urban system, the sound level shows a strong dependence on the observation point position, thus in the process of acoustical climate planning it is advisable to calculate the sound level in the vicinity of the building facade under investigation, at points corresponding to the windows' positions.

In the environmental noise model presented in the paper, a statistical character can be assumed for the highway model. The propagation model is determined, as is the urban system, without taking account of the atmospheric conditions. The level of mean acoustical energy (the sound equivalent level) is the aim of the calculation, as recommended by ISO for annoyance rating. Since it is related to subjective judgment, an accuracy of the order of 1 dB(A) is good enough. For this purpose the sound exposure of an individual vehicle drive-by, vehicle flow rate and its average speed are sufficient.

In spite of all the simplifications, it has been found in practice that fundamental effects connected with traffic noise propagation in an urban area can be quantitatively predicted by use of the PROP3 program.

REFERENCES

1. E. Walerian, M. Czechowicz and R. Janczur 1995 *Applied Acoustics* **44**, 291–324. Barriers' efficiency in different environment.
2. G. Kristensson and S. Strom 1978 *Journal of the Acoustical Society of America* **64**, 917–936. Scattering from buried inhomogeneities—a general three-dimensional formalism.
3. T. Terai 1980 *Journal of Sound and Vibration* **69**, 71–100. On calculation of sound fields around three dimensional objects by integral methods.
4. J. J. Brown, T. B. A. Senior and P. L. E. Uslenghi (editors) 1969 *Electromagnetic and Acoustical Scattering by Simple Shapes*. Amsterdam: North-Holland Company. See chapters 6 and 8.
5. A. Ciarkowski, J. Boersma and R. Mitrra 1984 *IEEE Transactions on Antennas and Propagation* **AP-32**, 20–29. Plane-wave diffraction by wedge—a spectral domain approach.
6. J. Chang-Sung, R. Jung and S. Sang-Yung 1984 *IEEE Transactions on Antennas and Propagation* **AP-32**, 61–69. Scattering by right angle dielectric wedge.
7. A. D. Rawlings 1987 *Proceedings of the Royal Society of London* **A411**, 265–283. Plane-wave diffraction by rational wedge.
8. K. Fujiwara, Y. Ando and Z. Maekawa 1977 *Applied Acoustics* **10**, 147–159. Noise control by barriers—Part I: Noise reduction by a thick barrier.
9. J. J. Hajek and L. Kawan 1980 *Proceedings of Internoise* '80, *Miami*, *FL*, 595–598. Effect of parallel highway noise barriers.
10. S. J. Hayek 1980 *Proceedings of Internoise* '80, *Miami*, *FL*, 585–588. Efficiency of double wall noise barriers.

11. D. Lohman 1980 *Journal of the Acoustical Society of America* **67**, 1974–1979. Fan noise by single and double-wall barriers.
12. Z. Maekawa 1985 *Archives of Acoustics* **10**, 369–382. Simple estimation method for noise reduction by variously shaped barriers.
13. M. Yuzuwa and T. Sone 1981 *Applied Acoustics* **14**, 65–73. Noise reduction by various shape barrier.
14. W. Bowlby, L. F. Cohn and R. A. Harris 1987 *Noise Control Engineering Journal* **28**, 40–53. A review of studies of insertion loss degradation for parallel highway noise barriers.
15. U. J. Kurze 1974 *Journal of the Acoustical Society of America* **55**, 504–517. Noise reduction by barriers.
16. Y. Sakurai and K. Ishida 1982 *Journal of the Acoustical Society of Japan* (*E*) **3**, 183–190. Multiple reflection between rigid plane panels.
17. Y. Sakurai and K. Ishida 1983 *Journal of the Acoustical Society of Japan* (*E*) **4**, 27–33. Multiple reflection between rigid curved panels.
18. Y. Sakurai and K. Ishida 1990 *Journal of the Acoustical Society of Japan* (*E*) **11**, 257–265. Multiple sound reflection between panels covered with reflection coefficients.
19. E. Walerian and R. Janczur 1985 *Institute of Fundamental Technological Research Reports* **25**. Theories of diffraction applied for description of acoustical field screen efficiency (in Polish).
20. H. G. Jonasson 1972 *Journal of Sound and Vibration* **25**, 577–585. Diffraction by wedge of finite acoustic impedance with applications to depressed roads.
21. S. I. Hayek 1990 *Applied Acoustics* **31**, 77–100. Mathematical modeling of absorbing highway noise barriers.
22. E. Walerian 1988 *Archives of Acoustics* **12**, 157–189. Half-plane wedge and right angle wedge as elements causing diffraction in urban area.
23. J. Borish 1984 *Journal of the Acoustical Society of America* **75**, 1827–1836. Extension of the image model to arbitrary polyhedra.
24. J. Kirszenstein 1984 *Applied Acoustics* **17**, 275–290. An image source computer model for acoustic analysis and electroacoustic simulation.
25. J. B. Allen and D. A. Berkeley 1975 *Journal of the Acoustical Society of America* **65**, 943–950. Image method for efficiently simulating small room acoustics.
26. A. D. Clayden, R. W. D. Culley and P. S. Marsh 1975 *Applied Acoustics* **8**, 1–12. Modelling traffic noise.
27. M. Genson and F. Santon 1979 *Journal of Sound and Vibration* **63**, 97–108. Prediction of sound field in room of arbitrary shape: the validity of the image source method.
28. G. Lemire and J. Nicolas 1989 *Journal of the Acoustical Society of America* **86**, 1845–1853. Aerial propagation of spherical sound waves in bounded spaces.
29. A. G. Galaitsis and W. N. Paterson 1976 *Journal of the Acoustical Society of America* **60**, 848–856. Prediction of noise distribution in various enclosures from free field measurements.
30. R. Janczur, E. Walerian and J. Ogłaza 1993 *Acustica* **78**, 154–162. Acoustical field in space with obstacles. Part I: Description of geometrical field.
31. E. Walerian and R. Janczur 1993 *Acustica* **78**, 210–219. Acoustical field in space with obstacles. Part II: Propagation between buildings.
32. E. Walerian 1993 *Acustica* **78**, 201–209. Multiple diffraction at edges and right angle wedges.
33. E. Walerian 1995 *Institute of Fundamental Technological Research Reports* **29**. Description of noise propagation in a built-up area.
34. P. Ambaud and A. Bergassol 1972 *Acustica* **27**, 291–298. Le problem du diedre en acoustique.
35. W. J. Hadden Jr. and A. D. Pierce 1981 *Journal of Acoustical Society of America* **69**, 1266–1276. Sound diffraction around screens and wedges for arbitrary point source locations.
36. A. D. Pierce 1974 *Journal of the Acoustical Society of America* **55**, 941–955. Diffraction of sound around corners and over wide barriers.
37. R. Janczur 1990 *Institute of Fundamental Technological Research Reports* **8**. Theoretical and scale-model investigation of a point source acoustical field in the presence of reflecting surfaces and screen. (Ph.D. Thesis, in Polish).
38. Y. Sakurai, E. Walerian and H. Morimoto 1990 *Journal of the Acoustical Society of Japan* (*E*) **11**, 257–265. Noise barrier for building facade.
39. W. Rubinowicz 1957 *Die Beugungswelle in der Kirchhoffschen Theorie der Beugung*. Warsaw: PWN Publishing House.
40. M. E. Delany, A. J. Rennie and K. M. Collins 1978 *Journal of Sound and Vibration* **56**, 325–340. A scale model technique for investigating traffic noise propagation.

41. M. YAMASHITA and K. YAMAMOTO 1990 *Applied Acoustics* **31**, 185–196. Scale model experiments for the prediction of road traffic noise and the design of noise control facilities.
42. B. RUDNO-RUDZINSKA 1994 *Scientific Papers of the Institute of Telecommunication and Acoustics of the Technical University of Wrocław No*. 75, *Monograph No*. 39, *Wrocław*. Modeling sound emission and propagation for prediction of the acoustic climate in urban environment (in Polish).
43. S. A. L. GLEGG and J. R. YOON 1990 *Journal of Sound and Vibration* **143**, 39–50. Determination of noise source heights, Part II. Measurement of the equivalent source height of highway vehicles.
44. R. KUCHARSKI 1990 *Ph.D. Thesis*, *Institute of Environmental Planning*, *Warsaw*. Prediction of acoustical climate parameters in dwelling depending on terrain and noise sources characteristic.
45. E. WALERIAN and R. JANCZUR 1991 *Institute of Fundamental Technological Research Reports* **32**. Model of highway as noise source.
46. R. MARKAREWICZ 1991 *Applied Acoustics* **34**, 37–50. Traffic noise in a built-up area.
47. R. MAKAREWICZ 1991 *Journal of Sound and Vibration* **148**, 409–422. Shielding of noise in a built-up area.
48. R. MAKAREWICZ 1993 *Journal of the Acoustical Society of Japan* (*E*) **14**, 301–306. Traffic noise in a built-up area influenced by the ground effect.
49. H. G. JONSSON 1973 *Journal of Sound and Vibration* **30**, 289–304. A theory of traffic noise propagation with application to L_{eq}.
50. H. KUTTRUFF 1982 *Journal of Sound and Vibration* **85**, 115–128. A mathematical model for noise propagation between buildings.
51. K. W. YEOW 1979 *Journal of Sound and Vibration* **67**, 219–229. Room acoustical model of external reverberation.
52. R. BULLEN 1979 *Journal of Sound and Vibration* **65**, 11–28. Statistical evaluation of the accuracy of external sound level predictions arising from models.
53. E. WALERIAN and R. JANCZUR 1994 *Archives of Acoustics* **19**, 201–225. Statistical description of noise propagation in a built-up area.
54. U. J. KURZE 1971 *Journal of Sound and Vibration* **18**, 171–195. Statistic of road traffic noise.
55. U. J. KURZE 1971 *Journal of Sound and Vibration* **19**, 167–177. Noise from complex road traffic.
56. P. K. ANDERSEN 1982 *Journal of Sound and Vibration* **80**, 267–274. Regulatory of traffic noise signal.
57. S. YAMAGUCHI 1989 *Applied Acoustics* **27**, 103–118. A prediction method of non-stationary road traffic noise based on fluctuation patterns of an average number of flowing vehicles.
58. Y. MITANI, M. OHTA and Y. XIAO 1988 *Journal of the Acoustical Society of Japan* (*E*) **9**, 47–51. A new estimation method of noise evaluation index, L_{eq}, by use of statistical information on the arbitrary type noise level fluctuation.
59. M. OHTA, A. IKUTA and N. TAKAKI 1990 *Acustica* **70**, 273–283. A prediction method of road traffic noise with non-Poisson type traffic flow based on the generalization of Stratonovich's theory for random point processes.
60. Z. JIPING 1992 *Noise Control Engineering Journal* **41**, 371–375. A study on the highway noise prediction model applicable to different traffic flow.
61. M. OHTA and Y. MITANI 1988 *Journal of the Acoustical Society of Japan* (*E*) **9**, 195–200. A practical prediction method using an elementary response wave form for the road traffic noise at a T-type intersection.
62. M. OHTA, S. MIYATA and O. NAGANO 1991 *Acustica* **73**, 263–270. A comparison of different fluctuation probability expressions based on the dB scale measurement of the noise environment of road traffic.
63. K. TAGAKI, K. HIRAMATSU and T. YAMAMOTO 1974 *Journal of Sound and Vibration* **36**, 417–431. Investigation on road traffic noise based on an exponentially distributed vehicles model—single line flow of vehicles with same acoustic power.
64. W. SHUO-XIAN 1986 *Proceedings of INTERNOISE*'86, *Cambridge*, *MA*, 739–742. A simple method for prediction curbside L_{10} level from a free multi-type vehicular flow.
65. A. IKUTA and M. OHTA 1985 *Proceedings of 2nd Western Pacific Regional Acoustic Conference*, *Hong-Kong*, 84–89. A systematic reduction method for the road traffic noise and ground vibration based on the arbitrary traffic flow model of non-Poisson type.
66. M. OHTA and Y. MITANI 1985 *Archives of Acoustics* **10**, 59–74. A fundamental study for predicting the urban street noise by use of the image method approach.
67. K. W. YEOW, N. POPPLEWELL and J. F. W. MACKAY 1978 *Journal of Sound and Vibration* **57**, 203–224. Shielding of noise from statistically stationary traffic flow by simple obstacles.